



Creep behavior and mechanical properties of Al-Li-S4 alloy at different aging temperatures

ZHOU Chang(周畅)^{1,2}, ZHAN Li-hua(湛利华)^{1,2}, SHEN Ru-lin(申儒林)^{1,2}, ZHAO Xing(赵兴)^{1,2}, YU Hai-liang(喻海良)^{1,2}, HUANG Ming-hui(黄明辉)^{1,2}, LI He(李贺)^{1,2}, YANG You-liang(杨有良)^{1,2}, HU Li-bin(胡立彬)^{1,2}, LIU De-bo(刘德博)³, HU Zheng-gen(胡正根)³

1. State Key Laboratory of High Performance Complex Manufacturing, Central South University, Changsha 410083, China;
2. College of Mechanical and Electrical Engineering, Central South University, Changsha 410083, China;
3. Beijing Institute of Aerospace Systems Engineering, Beijing 100076, China

© Central South University Press and Springer-Verlag GmbH Germany, part of Springer Nature 2020

Abstract: Creep age forming techniques have been widely used in aerospace industries. In this study, we investigated the effect of aging temperature (143 °C–163 °C) on the creep behavior of Al-Li-S4 aluminum alloy and their mechanical properties at room temperature. The mechanical properties were tested by tensile testing, and the microstructural evolution at different aging temperatures was examined by transmission electron microscopy. Results show that the creep strains and the room-temperature mechanical properties after creep aging increase with the aging temperature. As the aging temperature increases, the creep strain increases from 0.018% at 143 °C to 0.058% at 153 °C, and then to 0.094% at 163 °C. Within 25 h aging, the number of creep steps increases and the duration time of the same steps is shortened with the growth of aging temperatures. Therefore, the increase in aging temperatures accelerates the progress of the entire creep. Two main strengthening precipitates θ' (Al₂Cu) and T_1 (Al₂CuLi) phases were characterized. This work indicates that the creep strain and mechanical properties of Al-Li-S4 alloys can be improved by controlling aging temperatures.

Key words: Al-Li-S4 alloy; creep behavior; mechanical properties; aging temperature

Cite this article as: ZHOU Chang, ZHAN Li-hua, SHEN Ru-lin, ZHAO Xing, YU Hai-liang, HUANG Ming-hui, LI He, YANG You-liang, HU Li-bin, LIU De-bo, HU Zheng-gen. Creep behavior and mechanical properties of Al-Li-S4 alloy at different aging temperatures [J]. Journal of Central South University, 2020, 27(4): 1168–1175. DOI: <https://doi.org/10.1007/s11771-020-4357-3>.

1 Introduction

Aluminum lithium alloys exhibit many excellent properties such as low density, high elastic modulus, high strength, good fatigue resistance, corrosion resistance and welding performance, and are widely used in the aerospace field. Al-Li-S4 aluminum alloy is a third-generation Al-Cu-Li alloy,

and precipitation is the main strengthening mechanism. The addition of different trace elements in the alloy causes different compounds to form in the aging process. Modification of the microstructure distribution inside the alloy can affect the mechanical properties and usually improve the strength and toughness of the alloy.

ZHENG et al [1] reported that the precipitation sequence of Al-Cu-Li aluminum alloy is mainly

Foundation item: Project(2017YFB0306300) supported by National key R&D Program of China; Project(zzyikt2015-05) supported by the Project of State Key Laboratory of High Performance Complex Manufacture, China

Received date: 2019-01-23; **Accepted date:** 2020-02-16

Corresponding author: ZHAN Li-hua, PhD, Professor; Tel: +86-13974874472; E-mail: yjs-cast@csu.edu.cn; ORCID: 0000-0001-9419-4149; ZHAO Xing, PhD, Lecturer; Tel: +86-18773137235; E-mail: xingzhao@csu.edu.cn

determined by the Cu content of the alloy and the Cu/Li ratio. When the Cu content is between 2% and 5%, the precipitation sequence is supersaturated solid solution (SSS)→GP zone+ δ' → T_1 + θ' + δ' → T_1 and the main strengthening precipitates are GP zones and T_1 phase. From Al-Cu-Li ternary phase diagram, it can be realized that the second phases that may occur in the aluminum-lithium alloy are T_1 , θ' , δ' and S' . Some recent studies [2–5] revealed that the microscopic shapes of these strengthening phases are various, including sheet-like, disc-shaped, spherical, acicular and rod-shaped. There is ubiquitous precipitation of the metastable δ' phase and the lattice constant of this phase, 0.4038 nm, is only slightly smaller than that of the Al matrix, 0.404 nm, so that the δ' phase precipitates coherently in a spherical shape [4, 5]. The θ' phase, Al_2Cu , is a semicoherent metastable precipitate with a tetragonal structure of $a=0.404$ nm and $c=0.580$ nm and grows as thin plates on $\{001\}_\alpha$ planes [2, 3]. The T_1 phase has a lattice structure identical to the Al matrix, and consists of a stacking of Li-rich and Cu-rich layers along $\{111\}_\alpha$ planes [5]. Due to the different shape and main habit plane of the strengthening phase, the elastic distortion generated on the shear surface and the interface energy with the matrix are different, and the influence on the properties of the alloy is also diverse.

The creep aging forming technology combines creep forming and artificial aging of aluminum alloy. The creep behavior and aging precipitation strengthening characteristics of aluminum alloy under the joint action of stress and temperature are used to obtain satisfactory shape and good microstructure and properties [6–8]. ZENG et al [9] studied effects of aging temperature on microstructure, tensile and creep properties of ring rolled AZ80-Ag alloy, and found that with raising aging temperature, the tensile strength at ambient temperature reveals a descending tendency, whereas the creep resistance at 120–175 °C under 70–90 MPa exhibits an enhancement. ZHANG et al [10] investigated dynamic compression behavior of 6005 aluminum alloy aged at elevated temperatures, and reported that aging temperature has profound influence on generation of microstructure and resulting properties of the alloy, and dynamic stress–strain behavior exhibits an evident dependence on aging temperature which has an

influence on the initial microstructure. Some researchers carried out studies on the impacts of stress on the micro-precipitates and mechanical properties of Al-Cu-Li alloy in creep aging and found that the exterior stress can promote to form T_1 nano-precipitates, restrict both the coarsening of precipitates at grain boundaries and the formation of precipitation free zone [11]. LI et al [12] found that creep aging forming technology can enhance the mechanical properties and anti-corrosion properties of Al-Li alloy. ZHANG et al [13] found that creep aging promotes the nucleation of T_1 phase, resulting in a fine and dense distribution of precipitates in the matrix. Meanwhile, extensive investigations have been carried out on the influence of pre-deformation and stress on the micro-precipitates and creep behavior of Al-Cu-Li alloy [14, 15]. However, the effect of temperature on creep behavior, mechanical properties and micro-precipitates of Al-Cu-Li alloy is seldom reported.

The present work investigates the effect of aging temperature on creep aging behaviors of creep aging treated Al-Cu-Li alloy. The mechanical properties after the creep aging were tested by electronic universal testing machine, and the microstructure of samples after aging and the precipitate kinetics during the process were systematically studied using transmission electron microscopy (TEM). Two main strengthening precipitates θ' (Al_2Cu) and T_1 (Al_2CuLi) phases were characterized. These findings will enrich our understanding of microstructural evolution in the Al-Li-S4 alloy.

2 Materials and methods

The chemical composition of Al-Li-S4 alloy in this study was Al-3.64Cu-0.71Mg-0.69Li-0.36Zn-0.3Mn-0.12Zr-0.028Fe-0.026Ti-0.014Si (wt.%). The material was received in the form of a rolled plate with dimensions of 2 mm×400 mm×400 mm. The samples were solution treated at 530 °C for 80 min, followed by water quenching at room temperature. The error of temperature retained at ± 2 °C during solution treatment. Meanwhile, the time used for transferring specimen between furnace and water tank was less than 35 s. Thereafter, the samples were immediately installed in a furnace for creep aging test at 143–163 °C on

the RDL50® electronic creep test machine for 25 h under 220 MPa.

The dog bone-shaped creep samples had a 50 mm gage length, 15 mm gage width and 2 mm gage thickness. The tensile tests were carried out in a DDL100® electronic universal testing machine at a crosshead speed of 2 mm/min at room temperature. Microstructures of the creep aged Al-Cu-Li alloy were examined by TEM. The precipitation behavior of the alloy was analyzed based on bright field (BF) and high-angle annular dark field-scanning transmission electron microscopy (HAADF-STEM) images. The TEM and HRTEM observations were conducted in a FEI Titan G2 60-300 microscope operated at 300 kV. The TEM samples were prepared by mechanical grinding and electro-polishing in a solution of 75% CH₃OH and 25% HNO₃.

3 Results and discussion

3.1 Creep strain behaviour

Figure 1(a) shows the creep strain of Al-Li-S4 aluminum alloy as a function of aging time under the same stress and different temperature. The creep strain of the material rises significantly as the temperature increases from 143 °C to 163 °C. At the initial step of aging (0–1 h), the creep rate increases when the temperature increases. At the later state, the increase in temperature also increases the creep rate of the material. The final creep strain at 143 °C is 0.018%, and is raised to 0.058% at 153 °C and 0.094% at 163 °C, respectively. It can be seen that in the temperature range of 143–163 °C, the creep behavior of the material is enhanced as the temperature increases. The enhancement in the creep behavior (creep strain and creep rate) of Al-Li-S4 aluminum alloy is more pronounced for higher temperature. Moreover, it can be seen that within 25 h of aging, the number of creeping steps of the material also increases with the increase of temperature. A multi-step phenomenon of creep curve of the alloy appears at the temperature of 163 °C. A similar multi-step phenomenon emerges within 40 h aging time at 153 °C and 220 MPa as shown in Figure 1(c). It is suggested that a “multi-step” feature under the creep aging process in this range exists in Al-Li-S4 aluminum alloy under present situation. In Figure 1(a), with the increase of temperature, the duration of the second creep step (II-step) is shortened and the creep

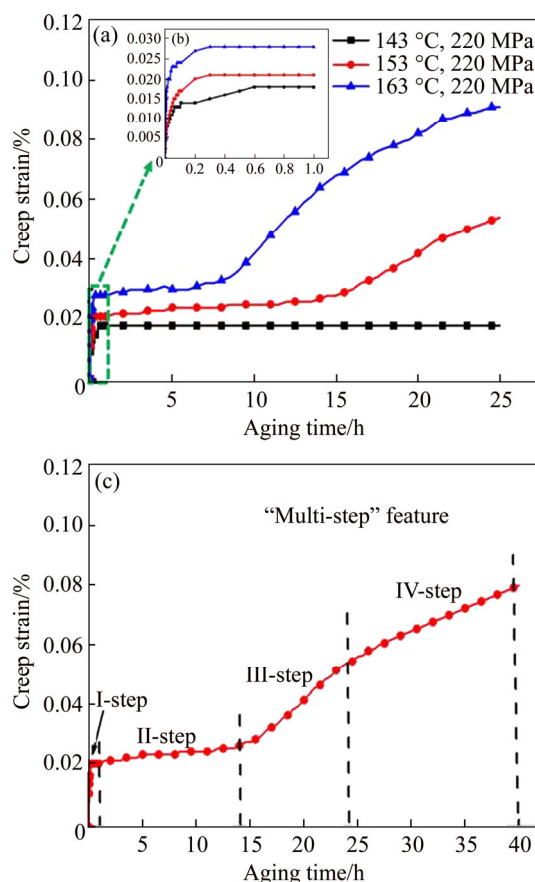


Figure 1 Creep behavior of Al-Li-S4 alloys: (a) Creep strain (ϵ) curves within 25 h of aging at different temperatures under 220 MPa; (b) Enlarged view of first 1 h of creep aging; (c) Creep strain (ϵ) curves within 40 h of aging at 153 °C under 220 MPa

progress speeds up to enter the third creep step (III-step). The increase in aging temperature also raises the creep rate of each step.

3.2 Mechanical properties

Figure 2 plots the strength and elongation of Al-Li-S4 alloys after creep aging at different temperatures (same stress and same time). It can be seen that in the temperature range of 143–163 °C, the strength of Al-Li-S4 aluminum alloys rises with the increase of temperature. The average values of yield strength (YS) and ultimate tensile strength (UTS) of the alloy increase from 310.4/455.2 MPa after creep aging at 143 °C to 425.6/514.5 MPa after creep aging at 153 °C, and 493.1/540.2 MPa after creep aging at 163 °C, respectively. The elongation (plasticity) of Al-Li-S4 aluminum alloy decreases (weakens) as the aging temperatures increase. As shown in Figure 2, the average value of elongation of the alloy decreases from 21.1% after

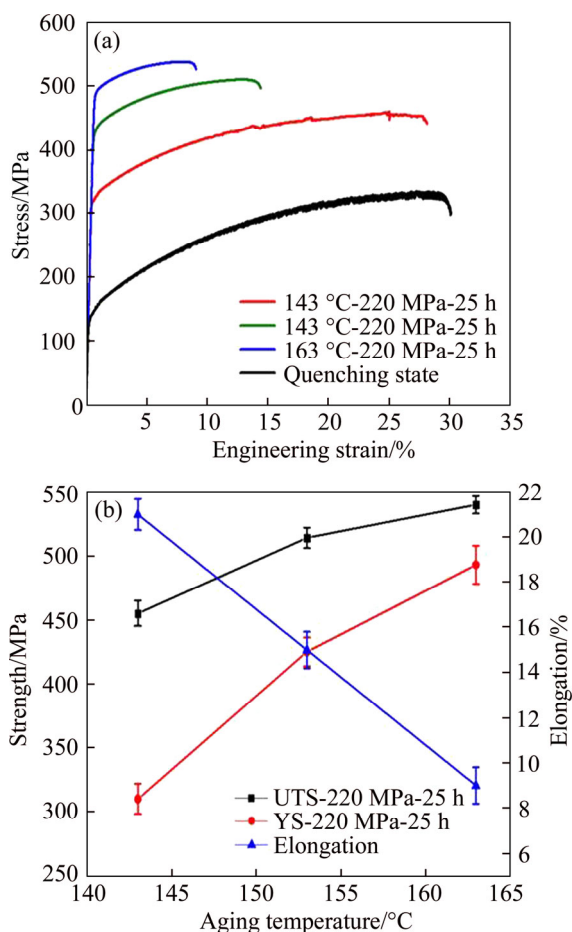


Figure 2 Mechanical properties of creep aged samples: (a) Stress–strain curves of one group; (b) Strength and elongation after creep aging at different temperatures under a given stress of 220 MPa for 25 h for Al-Li-S4 alloys

creep aging at 143 °C to 15.2% after creep aging at 153 °C and 8.8% after creep aging at 163 °C at the aging condition of 220 MPa and 25 h.

3.3 Microstructural investigation

Figure 3 presents the microstructure of the Al-Li-S4 aluminum alloy observed at room temperature, after creep aging at different temperatures under the stress of 220 MPa for 25 h. All the images were taken close to a $\langle 110 \rangle_{\text{Al}}$ zone axis.

The HAADF-STEM image in Figure 3(a₁), shows that most of the dislocations are piling up together, from which T_1 phase is nucleated. It is also detected that T_1 precipitates lie on the $\{1\bar{1}1\}$ and $\{\bar{1}11\}$ planes, which is consistent with the observations [13–17]. ZHANG et al [18] found that two variants of T_1 plate precipitate on $\{111\}_{\text{matrix}}$ planes and one variant of θ' plate on $\{100\}_{\text{matrix}}$

planes are parallel to $[110]_{\text{matrix}}$ direction and thus the cross section of the two phases are seen in TEM field when foil sample rotates to certain angle, and that the orientation relationship of θ' and T_1 phases is that the angle between θ' and T_1 phase is 125.3° and two variants of T_1 precipitate are 109.4° . Some researchers found that δ' and θ' are spherical, but δ' is the black dot and θ' is the white round particle (a little bit bigger) in the HAADF-STEM images with $[110]_{\text{matrix}}$ zone axis [16]. Furthermore, a small number of θ' precipitates are also observed on the $\{100\}_{\text{matrix}}$ planes, as well as bits of δ' phase. At the same time, it can be seen from the figure that there are quite a few large spherical dispersed β' precipitates (Al_3Zr) in the alloy. Since Zr is a slow-diffusing element in Al and its distribution is heterogenous, thus the density of β' phase is uneven [19]. The influence of β' on the property of the alloy is weak [20]. Bright-field TEM image presented in Figure 3(a₂) shows only small amounts of precipitates after stress aging at 143 °C for 25 h. This shows an under-aged alloy. The stress of 220 MPa produced volumes of dislocations in the matrix, which act as heterogenous nucleation sites for T_1 phase [11, 17]. The T_1 phase is nucleated from dislocations and a dense distribution of such precipitates is found close to dislocations with a diameter of around 50 nm, but no obvious homogeneous nucleation was found within dislocation-free zones at 143 °C after 25 h. Moreover, most of the T_1 phases are precipitated on one plane, but the orientation effect of T_1 phase cannot be derived because of the contrast.

As the aging temperature increased to 153 °C, the HAADF-STEM image in Figure 3(b₁) clearly shows the growth in the number and the size of T_1 phase. Both heterogenous nucleation from dislocations and homogeneous nucleation within dislocation-free zones are accelerated and a more dense and uniform distribution of T_1 phase is obtained on the $\{1\bar{1}1\}$ and $\{\bar{1}11\}$ planes. The number and size of θ' phase lying on $\{100\}_{\text{matrix}}$ planes also increase. The STEM image also shows a more dense distribution of spherical δ' phase. More precipitates also can be seen from Figure 3(b₂). Two out of four variants of T_1 phase can be seen along a $\langle 110 \rangle_{\text{Al}}$ zone axis and their number is a small increase, but the size is significantly increased than that at 143 °C with a diameter of around 100 nm. It is indicated that the increase of temperature

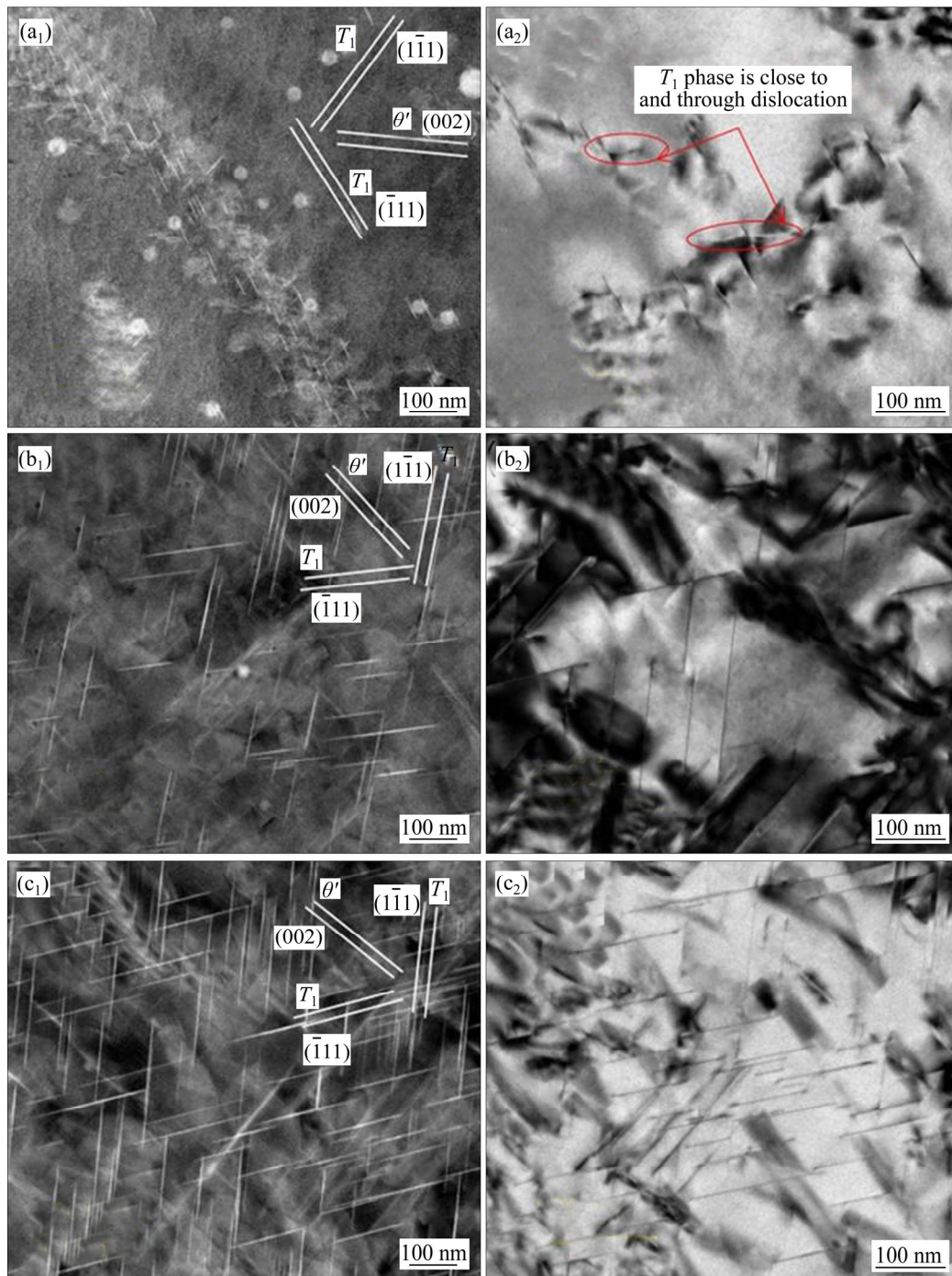


Figure 3 HAADF-STEM and bright field TEM images of Al-Li-S4 aluminum alloy at different aging temperatures under stress of 220 MPa after 25 h: (a₁) 143 °C, HAADF-STEM; (a₂) 143 °C, BF; (b₁) 153 °C, HAADF-STEM; (b₂) 153 °C, BF; (c₁) 163 °C, HAADF-STEM; (c₂) 163 °C, BF

enhances the nucleation and growth of the T_1 phase, thereby accelerating the entire creep aging progress.

When aging temperature further increased to 163 °C, almost no dislocations were observed in the alloy. The T_1 precipitates lying on both $\{1\bar{1}1\}$ and $\{\bar{1}11\}$ planes are densely distributed throughout the matrix. Only a minor fraction of θ' phase is present

while its size grows notably. And δ' phase is hardly seen in the matrix. The average diameter of T_1 phase at 163 °C is increased slightly compared to that at 153 °C, but the quantity is increased from about 90 at 153 °C to ~145 at 163 °C dramatically in the HAADF-STEM images, indicating an increase in the homogeneity of the distribution of T_1 precipitates. But no obvious thickening or

coarsening of the precipitates was observed, suggesting that the alloy has not reached peak state yet, which can also be confirmed by the continuous increased yield strength, as shown in Figure 2. The microstructure of Al-Li-S4 aluminum alloy in near-peak aged state is dominated by T_1 phase with minor θ' precipitates, which is in good agreement with previous observations [1, 11, 13, 15].

Our results showed that temperature plays an important role in the microstructural evolution of Al-Li-S4 aluminum alloy under creep aging deformation. The increase of temperature markedly changes the precipitation behaviors and leads to different creep aging behavior. HU et al [15] studied microstructural evolution of Al-Li-S4 alloys during aging creep and divided it into a few steps, i.e. I-step, II-step, III-step, IV-step, and concluded that I-step, a nucleation period of T_1 and θ' precipitates, and the dislocation hardening gradually reached a saturation level, which caused a fast decrease in the slope of ϵ curves; II-step, free growth of initial T_1 and θ' precipitates (that formed at I-step) in the length direction with solute-depletion, which is accompanied by the simultaneous nucleation of newer T_1 and θ' precipitates along the dislocations; III-step, continuous growth of previously-formed and newly-formed T_1 precipitates in the length direction, which is accompanied by the accelerating dissolution of θ' precipitates; IV-step, growth of T_1 in the thickness direction, marginal variation of θ' . Increasing the temperature of the creep aging process accelerates the diffusion of solute elements and improves the probability of collisions between elements, and reduces the energy required for the nucleation of precipitates (nucleation energy), therefore the phase transition process is accelerated. The evolution of microstructure is dominated by the heterogeneous nucleation of T_1 phase from dislocations and the precipitates are distributed close to dislocations inside the grain under the aging temperature of 143 °C. Because of the relatively low aging temperature of 143 °C, it could not contribute to continuous growth of previously-formed (that formed at II-step) and newly-formed T_1 precipitates in the length direction, so it stays in II-step. As the temperature of the whole process of creep aging increases to 153 °C, a more dense and uniform distribution of T_1 phase was observed due to the accelerated precipitation

process involving both heterogenous and homogeneous nucleation, moreover co-precipitation of θ' phase and δ' phase was activated.

It can be perceived that as the temperature increases, the nucleation energy decreases, the nucleation rate increases, leading to easy formation of T_1 , θ' and δ' phases. Rising temperature promotes dislocation motion, and dislocations are more evenly distributed inside the matrix, which provides heterogeneous nucleation sites for the T_1 phase and leads to uniform distribution of the T_1 phase. Under the multiphase precipitation, the strength of Al-Li-S4 aluminum alloy is improved, and the motion of dislocations contributes to the creep behavior of the alloy, as indicated by the increased creep strain of the alloy (Figure 1). When the temperature further rises to 163 °C, the main precipitates in the interior of the alloy are T_1 phases with a small amount of θ' phase, and the δ' phase is almost dissipated. Since the T_1 phase is the equilibrium phase and the θ' and δ' phases are the metastable phases, the change of volumetric free energy required to form the T_1 phase is larger than that of θ' and δ' phases. The larger volumetric free energy change caused the nucleation of T_1 phase to take precedence over the θ' phase at the dislocations of the matrix. When the temperature rises, the uniform distribution of dislocations continuously provides nucleation sites for the T_1 phase. And these uniformly distributed dislocations are likely to become vacant annihilation traps, reducing the number of vacancies, thereby inhibiting the formation of θ' phase and promoting the precipitation of the T_1 phase. And the nucleation and growth of the T_1 phase also leads to continuous consumption of Li elements in matrix and δ' phase [21, 22]. Among these main strengthening phases, the T_1 phase develops a high aspect ratio disk-like phase on the $\{111\}$ matrix, and the T_1 phase is regarded as the most important reinforcement precipitates in the aging Al-Li-Cu alloy [15]. As the temperature rises, the room-temperature mechanical properties after creep aging continue to increase. The motion of dislocations in the matrix also promotes creep behavior of the alloy and increases the creep strain, as shown in Figure 1.

4 Conclusions

- 1) The change of temperature in creep aging

treatment of an Al-Li-S4 alloy from 143 °C to 163 °C results in pronounced changes in creep behavior and micro-precipitates. The final creep strain of same stress level increases from 0.018% at 143 °C to 0.058% at 153 °C, and then to 0.094% at 163 °C.

2) The increase in temperature accelerates the progress of the entire creep aging. And within 25 h of creep aging, the number of creeping steps of the material also increases with the growth of temperature. The time of duration of ii-step stage is about 24 h under the aging temperature of 143 °C, and the temperature from 143 °C further rises to 153 °C, the time of duration of ii-step stage from 24 h is shortened to 12.5 h. When the temperature from 153 °C further rises to 163 °C, the time of duration of ii-step stage from 12.5 h is shortened to 6.5 h.

3) The precipitation of T_1 phase is distributed close to dislocations inside the grain under the aging temperature of 143 °C. As the temperature increases to 153 °C, a uniform distribution of T_1 phase and the co-precipitation of θ' phase and δ' phase is obtained. When the temperature further rises to 163 °C, main precipitates in the interior of the alloy are T_1 phases with a small amount of θ' phase, and the δ' phase is almost dissipated.

References

- [1] ZHENG Zi-qiao, LI Jin-feng, CHEN Zhi-guo, LI Hong-ying, LI Shi-chen, TAN Chen-yu. Alloying and microstructural evolution of Al-Li alloys [J]. The Chinese Journal of Nonferrous Metals, 2011, 21(10): 2237–2351. DOI: 10.19476/j.ysxb.1004.060 9.9.2011.10.004. (in Chinese)
- [2] YOSHIMURA R, J. KONNA T, ABE E J, HIRAGA K J. Transmission electron microscopy study of the evolution of precipitates in aged Al-Li-Cu alloys: the θ' and T_1 phases [J]. Acta Materialia, 2003, 51: 4251–4266. DOI: 10.1016/S1359-6454(03)00253-2.
- [3] DENG Yan-jun, HUANG Guang-jie, CAO Ling-fei, WU Xiao-dong, HUANG Li. Effect of ageing temperature on precipitation of Al-Cu-Li-Mn-Zr alloy [J]. Journal of Central South University, 2018, 25: 1340-1349. DOI: 10.1007/s11771-018-3830-8.
- [4] NOBLE B, THOMPSON G E. Precipitation characteristics of aluminium-lithium alloys [J]. Metal Science, 1971, 5(1): 114–120. DOI: 10.1179/030634 571790439333.
- [5] WILLIAMS D B, EDINGTON J W. The precipitation of δ' (Al_3Li) in dilute aluminium-lithium alloys [J]. Metal Science, 1975, 9(1): 529–532. DOI: 10.1179/030634575790 445143.
- [6] LI Xi-cai, ZHAN Li-hua. Unified constitutive modeling of creep aging behavior of AA2219 based on interaction of creep and aging interactive mechanism [J]. Journal of Central South University, 2017, 48(11): 2942–2948. DOI: 10.11817/j.issn.1672-720 7.2017.11.014.
- [7] STARKE JR E A, STALEY J T. Application of modern aluminum alloys to aircraft [J]. Woodhead Publishing Series in Metals and Surface Engineering, 1966, 32(2, 3): 131–172. DOI: 10.1533/97808 57090256.3.747.
- [8] ZHAN Li-hua, LIN Jian-guo, DEAN T A. A review of the development of creep age forming: Experimentation, modelling and applications [J]. International Journal of Machine Tools and Manufacture, 2011, 51(1): 1–7. DOI: 10.1016/j.ijmactools.2010. 08.007.
- [9] ZENG Gang, LIU Chu-ming, WANG Ying-chun, GAO Yong-hao, JING Shu-nong, CHEN Zhi-yong. Effects of aging temperature on microstructure, tensile and creep properties of ring rolled AZ80-Ag alloy [J]. Materials Science and Engineering A, 2018, 734: 59–66. DOI: 10.1016/j.msea.2018.07.061.
- [10] ZHANG Long, HE Hong, LI Shi-kang, WU Xiao-dong, LI Luo-xing. Dynamic compression behavior of 6005 aluminum alloy aged at elevated temperatures [J]. Vacuum, 2018, 155: 604–611. DOI: 10.1016/j.vacuum.2018.06.066.
- [11] HU Li-bin, ZHAN Li-hua, SHEN Ru-lin, LIU Zhi-lin, MA Zi-yao, LIU Jian, YANG Yin-ge. Effects of uniaxial creep ageing on the mechanical properties and microprecipitates of Al-Li-S4 alloy [J]. Materials Science and Engineering A, 2017, 668: 272–279. DOI: 10.1016/j.msea.2017.01.081.
- [12] LI H Y, KANG W, LU X C. Effect of age-forming on microstructure, mechanical and corrosion properties of a novel Al-Li alloy [J]. Journal of Alloys and Compounds, 2015, 640: 210–218. DOI: 10.1016/j.jallcom.2015.03.212.
- [13] ZHANG Jin, WANG Cheng, ZHANG Yong, DENG Yun-lai. Effects of creep aging upon Al-Cu-Li alloy: Strength, toughness and microstructure [J]. Journal of Alloys and Compounds, 2018, 764: 452–459. DOI: 10.1016/j.jallcom. 2018.06.103.
- [14] LI Y, SHI Z, LIN J, YANG Y L, HAUNG B M, CHUNG T F, YNAG J R. Experimental investigation of tension and compression creep-ageing behavior of AA2050 with different initial tempers [J]. Materials Science and Engineering A, 2016, 657: 299–308. DOI: 10.1016/j.msea.2016.01.074.
- [15] HU Li-bin, ZHAN Li-hua, LIU Zhi-lin, SHEN Ru-lin, YANG You-liang, MA Zi-yao, LIU Ming, LIU Jian, YANG Ying-ge, WANG Xun. The effects of pre-deformation on the creep aging behavior and mechanical properties of Al-Li-S4 alloys [J]. Materials Science and Engineering A, 2017, 703: 496–502. DOI: 10.1016/j.msea.2017.07.068.
- [16] DESCHAMPS A, DECREUS B, De GEUSER F, DORIN T, WEYLAND M. The influence of precipitation on plastic deformation of Al-Cu-Li alloys [J]. Acta Materialia, 2013, 61: 4010–4021. DOI: 10. 1016/j.actamat.2013.03.015.
- [17] CASSADA W A, SHIFLET G J, STARKE JR E A. Electron diffraction studies of Al_2CuLi [T_1] plates in an Al-2.4Li-2.4Cu-0.18Zr alloy [J]. Scripta Metallurgice, 1987, 21: 387–392. DOI: 10.1016/0036-9748(87)90234-1.
- [18] ZHANG Sai-fei, ZENG Wei-dong, YANG Wen-hua, SHI Chun-ling, WANG Hao-jun. Ageing response of a Al-Cu-Li 2198 alloy [J]. Materials and Design, 2014, 63: 368–374.

- DOI: 10.1016/j.matdes.2014.04.063.
- [19] DESCHAMPS A, GARCIA M, CHEVY J, DAVO B, De GEUSER F. Influence of Mg and Li content on the microstructure evolution of Al-Cu-Li alloys during long-term ageing [J]. *Acta Materialia*, 2017, 122: 32–46. DOI: 10.1016/j.actamat.2016.09.036.
- [20] HIROSAWA S, SATO T, KAMIO A. Effects of Mg addition on the kinetics of low-temperature precipitation in Al-Li-Cu-Ag-Zr alloys [J]. *Materials Science and Engineering A*, 1998, 242: 195–201. DOI: 10.1016/S0921-5093(97)00530-3.
- [21] GABLE B M, ZHUA W, CSONTOS A, STARKE E A Jr. The role of plastic deformation on the competitive microstructural evolution and mechanical properties of a novel Al-Li-Cu-X alloy [J]. *Journal of Light Metals*, 2001, 1: 1–14. DOI: 10.1016/S1471-5317(00)00002-X.
- [22] MA Pei-pei, ZHAN Li-hua, LIU Chun-hui, WANG Qing, LI He, LIU De-bo, HU Zheng-gen. Pre-strain -dependent natural ageing and its effect on subsequent artificial ageing of an Al-Cu-Li alloy [J]. *Materials Science and Engineering A*, 2019, 790: 8–19. DOI: 10.1016/j.jallcom.2019.03.072.
- (Edited by HE Yun-bin)

中文导读

时效温度对 Al-Li-S4 合金的蠕变行为和力学性能的影响

摘要：蠕变时效成形技术已经在航空航天领域得到了广泛的应用。本文研究了时效温度(143 °C~163 °C)对 Al-Li-S4 合金的蠕变行为和室温力学性能的影响。进行了力学性能拉伸测试和透射电镜下微观结构表征实验，结果表明：时效温度的升高，使得蠕变量及其对应的室温力学性能都会增加，具体表现为蠕变量从 143 °C 时的 0.018% 增加到 153 °C 时的 0.058%，进一步增加到 163 °C 时的 0.094%。在时效的 25 h 内，温度的升高使得蠕变阶段的数量增加，而对应的蠕变阶段保持的时间缩短。因此，时效温度的升高加速了蠕变时效进程。同时，对两种主要的强化相， θ' (Al_2Cu)相和 T_1 (Al_2CuLi)相进行了表征。研究表明，通过调控时效温度，可以获得 Al-Li-S4 合金的蠕变量和力学性能的改善。

关键词：Al-Li-S4 合金；蠕变行为；力学性能；时效温度